Magnetic properties of transition-metal surfaces: An energy comparison of different Hartree-Fock solutions*

H. Takayama,† Karen Baker, and Peter Fulde
Institut Max von Laue–Paul Langevin, 8046 Garching, Germany
(Received 16 April 1974)

A Hartree-Fock treatment of the surface of ferromagnetic transition metals will often lead to three self-consistent surface solutions. They correspond to different magnetic properties of the surface. We present here an energy comparison of these surface solutions. Two models, each having a different bulk density of states, are considered in order to study how sensitive our findings are to the shape of the bulk density of states. In many cases the solutions corresponding to a ferromagnetic and to an antiferromagnetic coupling of the surface layer to the bulk are found to have almost equal energy. This implies the possibility of low-energy magnetic surface excitations corresponding to a change of the surface layer from ferromagnetic to antiferromagnetic coupling or vice versa. For temperatures higher than this low-lying excitation energy but lower than the Curie temperature, the ferromagnetically and antiferromagnetically coupled states are equally populated and the surface layer has no net moment.

I. INTRODUCTION

An understanding of the surfaces of transition metals is not only of theoretical but also of practical interest mainly from the standpoint of their possible catalytic properties. Despite this, our knowledge of such surfaces is very limited, especially with respect to their magnetic properties. In a recent investigation by Fulde, Luther, and Watson[1] (hereafter referred to as paper I) an attempt was made to describe the different physical effects which are important in determining them. There the problem was divided into two parts. First, one must know how the d-hole count changes at the surface as compared with the one inside the bulk probe. It is, furthermore, important to know among how many subbands the surface d holes have to be distributed. Since the symmetry of the environment of a surface atom is lower than that of an atom inside the bulk, the number of subbands among which the d holes are distributed can be smaller at the surface.

After one has solved this problem—for example, by using the renormalized atom approach[2]—one is still left with the question of how such a surface layer couples to the ferromagnetic bulk. This problem was considered in paper I for a simple cubic (sc) lattice under the assumption that at the surface all d holes sit in one subband. (We expect this to be true in Ni where the threefold degenerate t_{2g} bands split at the surface into a low-lying filled doublet and a high-lying singlet which contains all the d holes.) It was found that with a ferromagnetic bulk there will be either one or three Hartree-Fock surface solutions, depending upon the d-hole count at the surface. When there is one solution, it corresponds to a ferromagnetic or an antiferromagnetic coupling of the surface to the bulk, depending upon fixed parameters. In the case of three solutions, there is an antiferromagnetic, a ferromagnetic, and an almost-vanishing surface magnetic moment.

The aim of the present investigation is twofold. First, an energy comparison is made in the case of multiple Hartree-Fock solutions. The circumstances under which the antiferromagnetic solution has the lowest energy are shown, and then excitation energies between the different solutions are calculated. Thus, it is found that the energy difference between the ferromagnetic and the antiferromagnetic surface solution can be very small.

Second, we want to determine the extent to which the results obtained depend upon the bulk density of states chosen to correspond to a sc lattice with nearest-neighbor interaction. We therefore modify the bulk density of states so that it more closely resembles the Ni bulk density of states, and then determine the resultant changes in the Hartree-Fock surface solutions.

In Sec. II we outline the free-energy calculations which provide a direct energy comparison of the different solutions. Section III contains the numerical results for a sc lattice with nearest-neighbor interactions. In Sec. IV it is shown to what extent a different bulk density of states changes the previous results. Section V contains a discussion of the results obtained, and Sec. VI is devoted to a summary and to the conclusions.

II. ENERGY CALCULATIONS

A. Model for the surface

The following considerations are made with Ni in mind. The five d orbitals can be divided into

a completely filled e_g doublet and a t_{2g} triplet which contains the d holes. Leaving the filled e_g orbitals out of all further considerations, we write the bulk Hamilton operator H^B in the form[3]

$$H^B = t \sum_{i,j,m,\sigma} a^\dagger_{im\sigma} a_{jm\sigma} + \sum_{i,m,\sigma} E^B_{t\sigma} a^\dagger_{im\sigma} a_{im\sigma} - H^B_{\mathrm{HF}} . \tag{1}$$

Here $a^\dagger_{im\sigma}$ denotes a creation operator of a t_{2g} electron in subband m ($m = 1, 2, 3$) and spin σ at site i. Furthermore, t is the hopping matrix element between neighboring sites i and j. The Hartree-Fock (HF) potential $E^B_{t\sigma}$ is the same for all three orbitals and is determined by

$$E^B_{t\sigma} = U(3n_{t-\sigma} + 2n_{t\sigma}) . \tag{2}$$

We have neglected the exchange energy here, since it is much smaller than the Coulomb energy U. $n_{t\sigma}$ is the bulk occupational number of any of the three t_{2g} orbitals. The last term in Eq. (1) is subtracted in order to prevent double counting of the interactions when the total energy is calculated. It is given by

$$\begin{aligned} H^B_{\mathrm{HF}} = {} & \frac{1}{2} \sum_{\substack{i,m,m'\sigma,\sigma' \\ (m=m',\,\sigma\neq\sigma')}} U\langle a^\dagger_{im\sigma} a_{im\sigma} a^\dagger_{im'\sigma'} a_{im'\sigma'}\rangle \\ & - \sum_{\substack{i,m,m'\sigma,\sigma' \\ (m=m',\,\sigma\neq\sigma')}} U\langle a^\dagger_{im\sigma} a_{im\sigma}\rangle\langle a^\dagger_{im'\sigma'} a_{im'\sigma'}\rangle \\ & = 3UN(n_t^2 + n_{t\uparrow} n_{t\downarrow}) . \end{aligned} \tag{3}$$

Here we have set n_t equal to $n_{t\uparrow} + n_{t\downarrow}$, and N equals the total number of atoms.

If a surface is introduced, several modifications arise which were discussed in detail in paper I. The following assumptions were made there which also apply here: (i) The hopping matrix element t does not change near the surface, except that it vanishes between the surface layer and the outside vacuum. (ii) The Coulomb integral U_S at the surface may be different from the bulk value U. (iii) The threefold degenerate bulk t_{2g} band splits at the surface into a high-lying singlet, which contains all of the d holes, and a low-lying doublet, which is assumed to be completely filled. (iv) The d-hole count is changed at the surface. Using the lowest approximation, the layer next to the surface layer is assumed to be unaffected by the presence of the surface.

In the presence of the surface, the Hamiltonian can then be written as

$$H = \bar{H}^B + H^S . \tag{4}$$

Here $\bar{H}^B$ is the bulk Hamiltonian given by Eq. (1) but with the inclusion of assumption (i) for the hopping term. The perturbation at the surface is described by the additional Hamiltonian H^S, where

$$H^S = \sum_{\substack{i,m,\sigma \\ i\in \text{surface}}} E_{m\sigma} n_{im\sigma} - H^S_{\mathrm{HF}} . \tag{5}$$

The Hartree-Fock potentials at the surface, $E_{m\sigma}$, are given by

$$E_{S\sigma} = E_S + U_S(2n_{D-\sigma} + n_{S-\sigma}) + 2U_S n_{D\sigma} - E^B_{t\sigma} \tag{6a}$$

and

$$E_{D\sigma} = E_D + U_S(2n_{D-\sigma} + n_{S-\sigma}) + U_S(n_{D\sigma} + n_{S\sigma}) - E^B_{t\sigma} . \tag{6b}$$

Here S and D refer to the singlet and doublet into which the t_{2g} bands split at the surface. The subtraction term H^S_{HF} is given by

$$\begin{aligned} H^S_{\mathrm{HF}} = N_{\parallel}[& U_S(n_D^2 + 2n_D n_S + 2n_{D\uparrow} n_{D\downarrow} + n_{S\uparrow} n_{S\downarrow}) \\ & - 3U(n_t^2 + n_{t\uparrow} n_{t\downarrow})] , \end{aligned} \tag{7}$$

where $n_{S,D} = n_{S,D\uparrow} + n_{S,D\downarrow}$, and $N_{\parallel}$ is the number of atoms in the surface layer.

With the assumption that the doublet is completely filled, Eqs. (6a) and (6b) simplify to

$$E_{S\sigma} = \tilde{E}_S + U_S n_{S-\sigma} , \tag{8a}$$

$$E_{D\sigma} = \tilde{E}_D + U_S n_S , \tag{8b}$$

where we have introduced

$$\begin{aligned} \tilde{E}_S &= E_S + 4U_S - E^B_{t\sigma} , \\ \tilde{E}_D &= E_D + 3U_S - E^B_{t\sigma} . \end{aligned} \tag{9}$$

Our aim will be to find self-consistently the singlet occupational numbers $n_{S\sigma}$ for known values of the parameters t, U, U_S, and $\tilde{E}_S$ as well as of $n_{t\sigma}$ for the bulk ferromagnetic state. In the case of multiple solutions, we want to compare their energies and to find which has the lowest energy.

B. Hartree-Fock equations for $n_{S\sigma}$

In order to calculate $n_{S\sigma}$ conveniently, we introduce the Green's function[4,5]

$$\begin{aligned} G_{m\sigma}(\omega, \vec{k}_{\parallel}; l, l') = {} & \int_0^\infty \frac{dt}{i} e^{i\omega t} \sum_n e^{i\vec{k}_{\parallel}\cdot\vec{R}_n} \\ & \times \langle [a_{ln\,m\sigma}(t), a^\dagger_{l'0m\sigma}]_+ \rangle . \end{aligned} \tag{10}$$

Here we have labeled the sites i and j by (l, n) and $(l', n' = 0)$, where $l \geq 0$ denotes the different layers parallel to the surface and n labels the different atoms within a layer. The surface itself is labeled by $l = 0$. $\vec{k}_{\parallel}$ is the momentum parallel to the surface. $G_{m\sigma}(\omega, \vec{k}_{\parallel}; 0, 0)$ is easily obtained for a sc lattice[5] and is given by

$$G_{m\sigma}(\omega, \vec{k}; 0, 0) = \frac{g_{t\sigma}(\omega, \vec{k}_{\parallel})}{1 + th_{t\sigma}(\omega, \vec{k}_{\parallel}) - E_{m\sigma} g_{t\sigma}(\omega, \vec{k}_{\parallel})} , \tag{11}$$

where

$$g_{t\sigma}(\omega, \vec{k}_{\parallel}) = N_{\perp}^{-1} \sum_{k_z} (\omega - \epsilon_{\vec{k}_{\parallel}} - 2t\cos k_z - E_{t\sigma}^{B})^{-1} , \tag{12}$$

$$h_{t\sigma}(\omega, \vec{k}_{\parallel}) = N_{\perp}^{-1} \sum_{k_z} \cos k_z (\omega - \epsilon_{\vec{k}_{\parallel}} - 2t\cos k_z - E_{t\sigma}^{B})^{-1} , \tag{13}$$

and $\epsilon_{\vec{k}_{\parallel}} = 2t(\cos k_x + \cos k_y)$. $N_{\perp}$ is the total number of layers. The lattice constant has been set equal to unity and the surface was chosen perpendicular to the z axis. The surface density of states for the singlet can then be written as

$$\rho_{S\sigma}(\omega) = -\frac{1}{\pi N_{\parallel}} \sum_{\vec{k}_{\parallel}} \mathrm{Im} G_{S\sigma}(\omega, \vec{k}_{\parallel}; 0, 0) , \tag{14}$$

and the surface singlet occupation number as

$$n_{S\sigma} = \int_{-\infty}^{\epsilon_F} d\omega \, \rho_{S\sigma}(\omega) , \tag{15}$$

where ϵ_F is the Fermi energy of the system and $N_{\parallel}$ is the number of atoms within one layer.

The bulk quantity $n_{t\sigma}$ is determined from $G_{m\sigma}(\omega, \vec{k}_{\parallel}; l, l)$ by choosing l very large. The effect of H^S is then quite small. The flow of charge to the surface actually affects the bulk by a correction of order $N_{\perp}^{-1}$. For $l \gg 1$

$$G_{m\sigma}(\omega, \vec{k}_{\parallel}; l, l) \simeq g_{t\sigma}(\omega, \vec{k}_{\parallel}) . \tag{16}$$

Hence, the bulk density of states is given by

$$\rho_{t\sigma}(\omega) = -\frac{1}{\pi N_{\parallel}} \sum_{\vec{k}_{\parallel}} \mathrm{Im} g_{t\sigma}(\omega, \vec{k}_{\parallel}) , \tag{17}$$

where $g_{t\sigma}$ is determined by H^B and is given by Eq. (12).

C. Energy comparison

In order to compare the energy of different Hartree-Fock surface solutions, we adopt the following procedure. First, we calculate the shift of the thermodynamic potential due to the perturbation Hamiltonian H^S. This is done by diagrammatic method, i.e., a Green's-function method. Then we take the limit of zero temperature. An important advantage of this method is that feedback effects of the surface on the bulk properties are automatically taken into account.[6] Though they are not important for a determination of $n_{S\sigma}$, they must be taken into account when added up for an energy comparison between different states. The difference in the thermodynamical potentials due to a perturbation H^S is given by[7]

$$\Omega - \Omega_0 = -T(\langle S \rangle_c^0 - 1) . \tag{18}$$

Here S denotes the S matrix due to H^S. The index c indicates that only connected diagrams have to be taken while the degree sign refers to a thermodynamic average over unperturbed states. In the following argument, we neglect the effect of electrons in the surface doublet subbands. The justification for this is given in Appendix B. So Eq. (18) reduces to

$$\Omega - \Omega_0 = T \sum_{\omega_n} \sum_{\vec{k}_{\parallel}\sigma} \{E_{S\sigma} G_{t\sigma}^0(\omega_n, \vec{k}_{\parallel}; 0, 0) + \tfrac{1}{2}[E_{S\sigma} G_{t\sigma}^0(\omega_n, \vec{k}_{\parallel}; 0, 0)]^2 + \tfrac{1}{3}[E_{S\sigma} G_{t\sigma}^0(\omega_n, \vec{k}_{\parallel}; 0, 0)]^3 + \cdots\} - H_{\mathrm{HF}}^S . \tag{19}$$

$G_{t\sigma}^0(\omega_n, \vec{k}_{\parallel}; l, l)$ denotes the Green's function given by Eq. (11) in the absence of H^S, that is, for $E_{m\sigma} = 0$, and is written in terms of Matsubara frequencies $[\omega_n = 2\pi T(n + \frac{1}{2})]$. If the zero-temperature limit is taken, $\Omega - \Omega_0$ goes over into ΔE, which is the energy shift of the ground state. The sum in Eq. (19) can be simply performed by analytical continuation, and one obtains

$$\Delta E = \frac{1}{\pi} \sum_{\vec{k}_{\parallel}, \sigma} \int_{-\infty}^{\epsilon_F} d\omega \, \mathrm{Im}\{\ln[1 - E_{S\sigma} G_{t\sigma}^0(\omega, \vec{k}_{\parallel}; 0, 0)]\} - N_{\parallel}[U_S n_{S\uparrow} n_{S\downarrow} - 3U(n_t^2 + n_{t\uparrow} n_{t\downarrow})] . \tag{20}$$

Here we can neglect small corrections to ϵ_F and $n_{t\sigma}$ due to the presence of the surface, since the feedback effects of the surface mentioned above are properly taken into account in that equation. Actually, one can show that the condition $\partial \Delta E / \partial n_{S\sigma} = 0$ leads to the Hartree-Fock equations (11)–(15) including the lowest-order terms in $N_{\perp}^{-1}$.

Since we want to compare energies of different states which are distinct only with respect to $n_{S\sigma}$, we rewrite Eq. (20) after partial integration as

$$\frac{\Delta E}{N_{\parallel}} = -\frac{1}{\pi} \sum_{\vec{k}_{\parallel}, \sigma} \int_{-\infty}^{\epsilon_F} d\omega \, (\omega - \epsilon_F) \times \frac{\partial}{\partial \omega} \mathrm{Im}[\ln G_{S\sigma}^{-1}(\omega, \vec{k}_{\parallel}; 0, 0)] - U_S n_{S\uparrow} n_{S\downarrow} + \mathrm{const}, \tag{21}$$

where the constant term contains only quantities which are independent of $n_{S\sigma}$.

III. NUMERICAL RESULTS

We present in this section the numerical results in a way that enables us to compare readily in Sec. IV the changes caused by a different choice of the bulk density of states.

A. Bulk density of states

We define the two-dimensional density of states $\rho_{\parallel}(\epsilon)$ by

$$\rho_{\parallel}(\epsilon) = N_{\parallel}^{-1} \sum_{\vec{k}_{\parallel}} \delta(\epsilon - \epsilon_{\vec{k}_{\parallel}}) . \tag{22}$$

Within the parabolic band approximation, $\rho_{\parallel}(\epsilon)$ is given by

$$\rho_{\parallel}(\epsilon) = \begin{cases} (8t)^{-1} & \text{for } -4t < \epsilon < 4t \\ 0 & \text{otherwise} . \end{cases} \tag{23}$$

This implies for the bulk density of states $\rho_B(x)$ [see Eq. (17)]

$$\rho_B(x) = -\frac{1}{8\pi t} \operatorname{Im} \int_{-2}^{+2} dy \, [(x-y)^2 - 1]^{-1/2} , \tag{24}$$

where $y = \epsilon/2t$ and x denotes the energy in units of $2t$. For later comparison we have plotted $\rho_B(x)$ in Fig. 1.

B. Surface density of states

The surface density of states given by Eq. (14) is written

$$\begin{aligned} \rho_{S\sigma} &\equiv \rho_{\alpha}(x) \\ &= -\frac{1}{4\pi t} \operatorname{Im} \int_{-2}^{+2} dy \, \frac{1}{[(x-y)^2 - 1]^{1/2} + (x-y) - \alpha} \\ &= \rho_{\alpha}^{\mathrm{NR}}(x) + \rho_{\alpha}^{\mathrm{R}}(x) . \end{aligned} \tag{25}$$

Here $\alpha = E_{S\sigma}/t$ characterizes the surface potential. $\rho_{\alpha}(x)$ can be divided into two terms. The first arises from the imaginary part of the square root in the denominator of the integrand and is called the nonresonant part $\rho_{\alpha}^{\mathrm{NR}}(x)$. The second term $\rho_{\alpha}^{\mathrm{R}}(x)$ results from the poles of the integrand if $|\alpha| > 1$. In analogy with a resonance level appearing in the one-impurity problem, we are referring to this contribution as a two dimensional surface resonance density of states $\rho_{\alpha}^{\mathrm{R}}(x)$. It is square in shape, with the center at $x_c = (\alpha^2+1)/2\alpha$ and with a width and height of $4(\times 2t)$ and $(\alpha^2-1)/8\alpha^2 t$, respectively. The explicit expression for $\rho_{\alpha}^{\mathrm{NR}}(x)$ is given in Appendix A by Eq. (A1). We have plotted in Fig. 1 $\rho_{\alpha}(x)$ with $\alpha = 0$ and 0.95. (The characteristic features of $\rho_{\alpha}(x)$ for $|\alpha| > 1$ were discussed in I.) Here it is important to note that $\rho_{\alpha}^{\mathrm{NR}}(x)$ is nonvanishing in the same energy range as is the bulk density of states $\rho_B(x)$, whereas $\rho_{\alpha}^{\mathrm{R}}(x)$ has a nonvanishing value also outside this regime.[4]

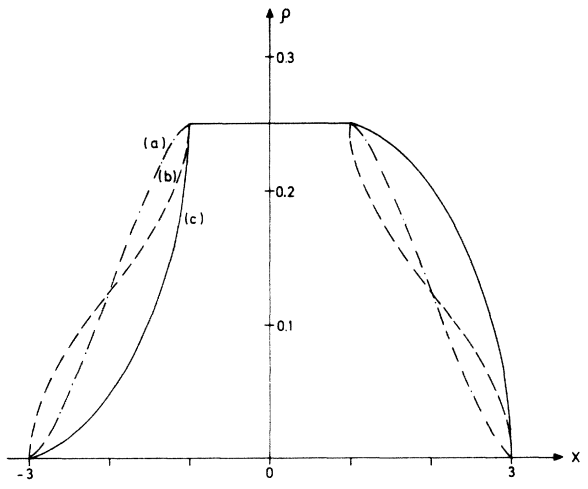

FIG. 1. Densities of states (a) $\rho_B(x)$, (b) $\rho_{\alpha=0}(x)$, and (c) $\rho_{\alpha=0.95}(x)$. The energy x is in units of $2t$; ρ is in units of $(2t)^{-1}$.

C. Surface occupational number

For a given surface potential α, $n_{S\sigma}$ can be determined with the help of Eqs. (15) and (25) once the Fermi energy ϵ_F is known. We require for paramagnetic Ni 0.1 holes per spin direction for each of the three t_{2g} subbands. This leads to $\epsilon_F^P = 1.6865$, again in units of $2t$. For the ferromagnetic state of Ni, we assume that the spin-up band is completely filled while the spin-down band contains all the d holes. Hence[8]

$$\begin{aligned} &\epsilon_{F\downarrow} = 1.2044 , \\ &\epsilon_{F\uparrow} = 3.0 + 1.2(U - U_0), \quad U \geq U_0 . \end{aligned} \tag{26}$$

Here we have expressed the Coulomb energies U and U_0 in units of the total bandwidth $12t$. $U_0 = 1.5$ denotes the critical Coulomb energy above which we are in the regime of strong ferromagnetism where one spin band is completely filled. Numerical results for $n_{S\sigma}$ are shown in Fig. 2 for $U = \frac{4}{3}U_0$, which implies $\epsilon_{F\uparrow} = 3.60$. Also shown for comparison are the corresponding curves for $U = U_0$ ($\epsilon_{F\uparrow} = 3.00$) which were calculated before in paper I.

D. Solutions of the Hartree-Fock equations and energy comparison

We have solved the Hartree-Fock equations numerically by combining Eq. (8a) with the results shown in Fig. 2. The quantity $\tilde{E}_S$ is determined by requiring a fixed value for $n_{S\uparrow} = n_{S\downarrow} = n_S^P$ which can be estimated, for instance, by applying the renormalized atom approach.[1] Here we leave n_S^P as a parameter. Figure 3 shows some numerical results applicable to the case of Ni. The magnetization $M = n_{S\uparrow} - n_{S\downarrow}$ is plotted as a function of n_S^P. The quantity $(n_S^P - 0.9)$ corresponds to the "charge transfer" of paper I. In order to see the dependence of the results on the absolute magnitude of $U = U_S$, we have plotted in Fig. 3(A) curves for $U = U_S = \frac{4}{3}U_0$ and $U = U_S = U_0$. Figure 3(B) shows the dependence on the ratio U_S/U choosing a

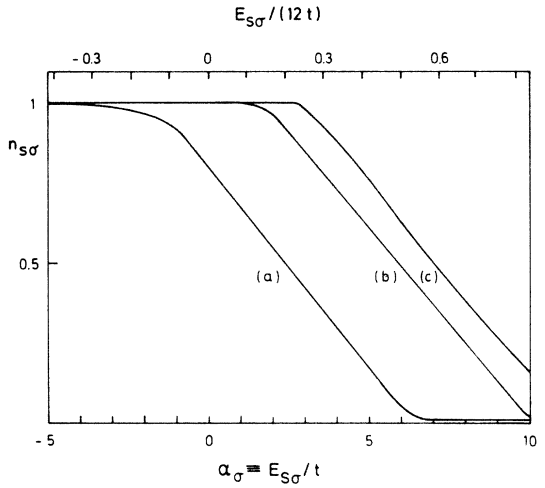

FIG. 2. Surface occupation number n_σ as a function of the surface potential $\alpha_\sigma = E_{S\sigma}/t$. For convenience we show on the upper scale the energy in units of the total bandwidth $12t$. Curve (a) corresponds to the minority spin band with $\epsilon_{F\downarrow} = 1.20$. Curves (b) and (c) correspond to the majority spin band with $\epsilon_{F\uparrow} = 3.00$ and $\epsilon_{F\uparrow} = 3.60$, respectively.

fixed value $U/U_0 = 1.06$. In the case of three Hartree-Fock solutions, the ones with the largest and smallest M are called the ferromagnetic and antiferromagnetic solution, while the third one is referred to as the paramagnetic solution. It should be mentioned that curve A of Fig. 3 in paper I is in error and has the form shown here.

Within the present model the shift of the ground-state energy due to the surface magnetization can be calculated analytically. Details of this calculation are given in Appendix B. Here we present merely the results. In Fig. 4 the energy differences between the ferromagnetic and paramagnetic solutions, $E(\mathrm{F}) - E(\mathrm{P})$, and between the antiferromagnetic and ferromagnetic solutions, $E(\mathrm{AF}) - E(\mathrm{F})$, are plotted as a function of n_S^P for $U = U_S = U_0$ and $U = 1.06U_0$, $U_S = 0.63U$. By considering other cases as well, such as $U = U_S = \frac{4}{3}U$ and $U = 1.06U_0$, $U_S = 0.81U$, one notices that the general features of the curves are the following: As n_S^P decreases from unity, the three solutions appear at a value n_S^{cr} which is about 0.9. The lowest energy solution below n_S^{cr} corresponds to the single solution above n_S^{cr}. If it is the ferromagnetic solution (three cases in Fig. 3), then the antiferromagnetic solution becomes lowest in energy when $n_S^P \leq 0.7 \sim 0.6$. On the other hand, if the single solution is antiferromagnetic, this solution stays lowest in energy for all values of n_S^P. In all cases the paramagnetic solution is highest in energy, and $|E(\mathrm{F}) - E(\mathrm{P})| \gg |E(\mathrm{AF}) - E(\mathrm{P})|$ holds true except in the close vicinity of n_S^{cr}.

From these investigations we see at once that decreasing U_S/U tends to favor the antiferromagnetic solution. Such a tendency has already been

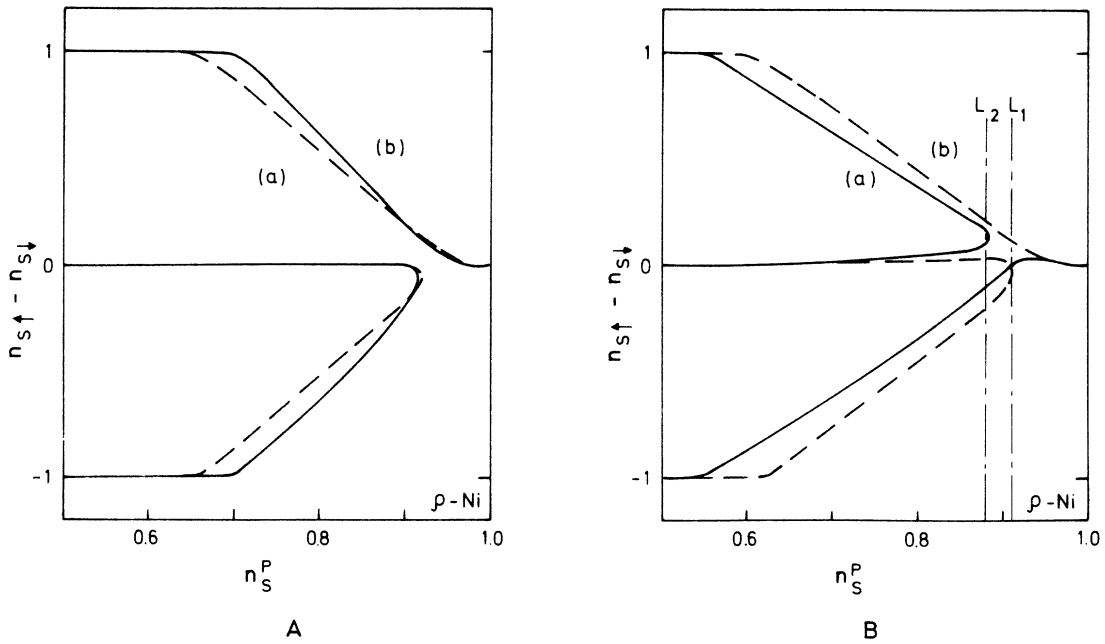

FIG. 3. Surface magnetization $n_{S\uparrow} - n_{S\downarrow}$ versus n_S^P. Shown in (A) are the cases (a) $U = U_S = U_0$, (b) $U = U_S = 1.33U_0$; in (B) are (a) $U = 1.06U_0$, $U_S = 0.63U$, (b) $U = 1.06U_0$, $U_S = 0.81U$. For case (b) of (B), L_1 and L_2 indicate at which values of n_S^P we draw the energy vs magnetization curves in Fig. 9.

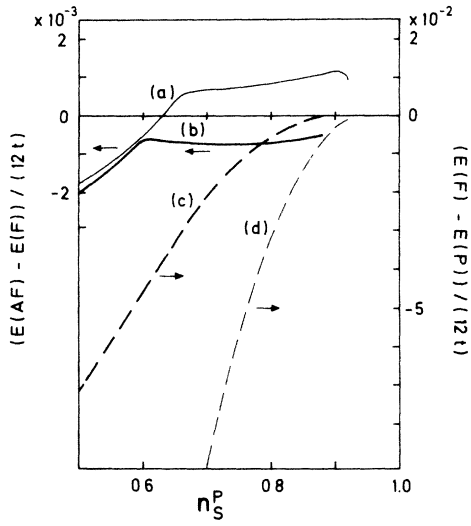

FIG. 4. Energy differences $E(\mathrm{F})-E(\mathrm{P})$ and $E(\mathrm{AF})-E(\mathrm{F})$ are shown by the broken and solid lines, respectively. (b) and (c) are for the case $U=1.06U_0$, $U_S=0.63U$ while (a) and (d) have $U=U_S=U_0$. The energy in this figure is in units of the total bulk bandwidth. Note the difference in scales for $E(\mathrm{F})-E(\mathrm{P})$ and $E(\mathrm{AF})-E(\mathrm{F})$.

pointed out in paper I. Most interesting is the extremely small energy difference between the ferromagnetic and antiferromagnetic solutions. When we assume 2 eV for the total bandwidth, $E(\mathrm{AF})-E(\mathrm{P})$ is smaller than 10^{-3} eV, i.e., 10 °K. This opens up the possibility of low-lying magnetic surface excitations corresponding to a switchover of the surface layer from ferromagnetic to antiferromagnetic coupling to the bulk or vice versa.

IV. VARIATION OF THE BULK DENSITY OF STATES

The aim of this section is to study how sensitive the numerical results obtained so far are to the chosen form of the bulk density of states that represents a sc lattice with nearest-neighbor interactions in the parabolic approximation.

A. Bulk density of states

In order to approach the bulk density of states of Ni more closely,[9] we introduce instead of Eq. (23) the following form for the two-dimensional density of states:

$$\bar{\rho}_{\parallel}(\epsilon)=\begin{cases} b/t & \text{for } -4t<\epsilon\leq 2\beta t \\ a/t & \text{for } 2\beta t<\epsilon<4t \\ 0 & \text{otherwise.} \end{cases} \tag{27}$$

The bar distinguishes the present quantities from the ones considered earlier. β and $r\equiv a/b$ are parameters which are chosen to approximate the Ni bulk density of states more closely. In Fig. 5(A) we show $\bar{\rho}_B(x)$ for $\beta=1$ and $r=7$. We intentionally write $\bar{\rho}_{\parallel}(\epsilon)$ in what appears to be a complicated manner since this allows the calculations of the energy shifts still to be performed analytically.

B. Surface density of states

The surface density of states is evaluated as before. Here, we show only the final results for $\alpha=0$ and 0.69 in Fig. 5(A) and for $\alpha=-2.15$ and 2.66 in Fig. 5(B). The parameter α's in Fig. 5(B) are those of the majority and minority electrons for the antiferromagnetic solution with $U=1.06U_0$, $U_S=0.63U$, and with $n_S^P=0.82$ (indicated by the cross in Fig. 7). Figure 5(B) clearly shows the importance of surface resonance levels to obtain the antiferromagnetic solution.

C. Surface occupational number

The Fermi energy for the paramagnetic state of Ni is now given by $\epsilon_F^P=2.0331$ and for the ferromagnetic state by

$$\epsilon_{F\downarrow}=1.8664, \quad \epsilon_{F\uparrow}=3.0+1.2(U-U_0), \quad U\geq U_0.$$

The critical Coulomb energy U_0 necessary for strong ferromagnetism to occur is now given by $U_0=0.9447$. This smaller value of U_0 is due to the fact that $\bar{\rho}_B(x)$ has a larger value close to the upper band edge than $\rho_B(x)$. $n_{S\sigma}$ is calculated as a function of α as previously, and the results are shown in Fig. 6. We have again chosen values for $\epsilon_{F\uparrow}$ corresponding to $U=U_0$ and $\frac{4}{3}U_0$, and for $\epsilon_{F\downarrow}$ corresponding to $U\geq U_0$. One notices a distinct difference between Figs. 6 and 2 due to the occurrence of a discontinuous change in slope in the curves of Fig. 6, which is, of course, due to the discontinuity in $\bar{\rho}_{\parallel}(\epsilon)$.

D. Solutions of the Hartree-Fock equations and energy comparison

Self-consistent solutions of $n_{S\sigma}$ for the ferromagnetic bulk state, and the energy differences $E(\mathrm{F})-E(\mathrm{P})$ and $E(\mathrm{AF})-E(\mathrm{F})$, are plotted in Figs. 7 and 8, respectively. (The method of calculation of the energy differences is discussed in Appendix B.) The chosen values for the parameters U and U_S are the same as those in Figs. 3 and 4. When compared with the previous results, the over-all behavior of the surface magnetization, as well as the behavior of the energy difference curves, is similar for the two cases. The small differences in the magnetization curves are easily understood when we compare the $n_{S\sigma}$ vs α curves in Figs. 2

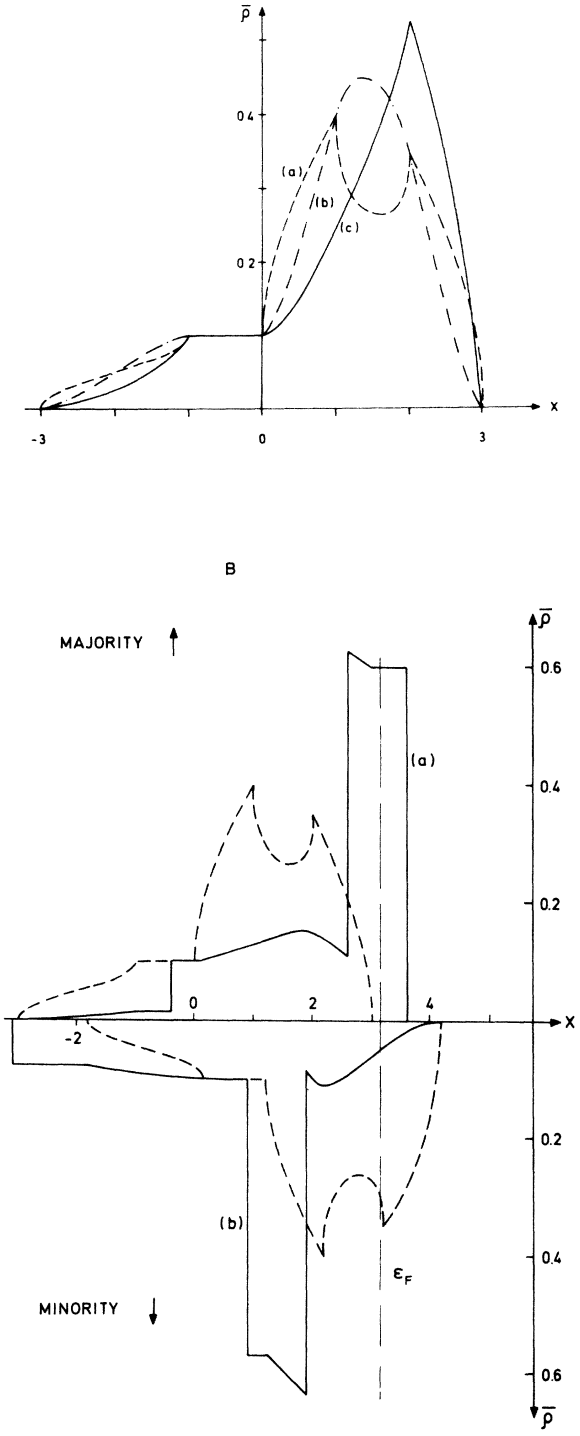

FIG. 5. (A) Densities of states (a) $\bar{\rho}_B(x)$, (b) $\bar{\rho}_{\alpha=0}(x)$, and (c) $\bar{\rho}_{\alpha=0.68}(x)$. This may be compared with Fig. 1. (B) Density of state $\bar{\rho}_\sigma(x)$ for the antiferromagnetic solution with $U=1.06U_0$, $U_S=0.63U$, and $n_S^P=0.82$ (indicated by a cross in Fig. 7 B). For this solution we obtain (a) $\alpha_\uparrow=2.66$ and (b) $\alpha_\downarrow=-2.15$. The broken line is the bulk density of states $\bar{\rho}_{B\sigma}(x)$. The vertical line indicates ϵ_F.

and 6. Most important is the fact that the ferromagnetic solution is more stable in this case than it was in the previous case. Actually, we cannot obtain the single antiferromagnetic solution even for $U_S/U=0.63$, $U=1.06U_0$. Furthermore, the energy difference $E(\mathrm{AF})-E(\mathrm{F})$ in the present case is several times larger than it was before, but is still very small.

One more small difference is the fact that for $U=1.06U_0$, $U_S=0.63U$ the antiferromagnetic solution is highest in energy in the region of $n_S^P \simeq n_S^{cr}$. In order to obtain a better understanding of this feature, we have tried to calculate the energy versus magnetization curves. Energies corresponding to other than the Hartree-Fock solutions are evaluated by means of Eq. (21) using arbitrary values for $n_{S\uparrow}$ or $n_{S\downarrow}$ (the details are found in Appendix B). In usual cases, in which the paramagnetic solution is highest in energy, the double minima in energy correspond to the antiferromagnetic and ferromagnetic solutions. They are shown in Figs. 9(A) and 9(B). These figures also demonstrate how the double minima develop as n_S^P decreases. On the other hand, in the case in which the antiferromagnetic solution is highest in energy, the situation is not as clear. This is shown in Fig. 9(C). The Hartree-Fock solution corresponds to the intersection of the two curves

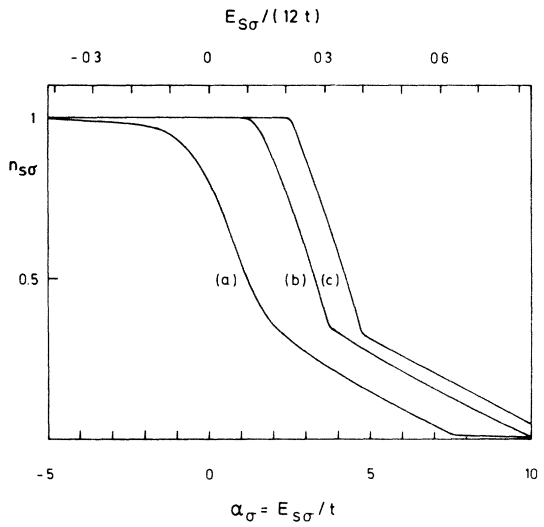

FIG. 6. Surface occupation number as a function of the surface potential $\alpha_\sigma=E_{S\sigma}/t$ calculated from $\bar{\rho}_{\alpha\sigma}(x)$. Curve (a) corresponds to the minority spin band with $\epsilon_{F\downarrow}=1.87$. Curves (b) and (c) correspond to the majority spin band with $\epsilon_{F\uparrow}=3.00$ and $\epsilon_{F\uparrow}=3.38$, respectively. This may be compared with Fig. 2.

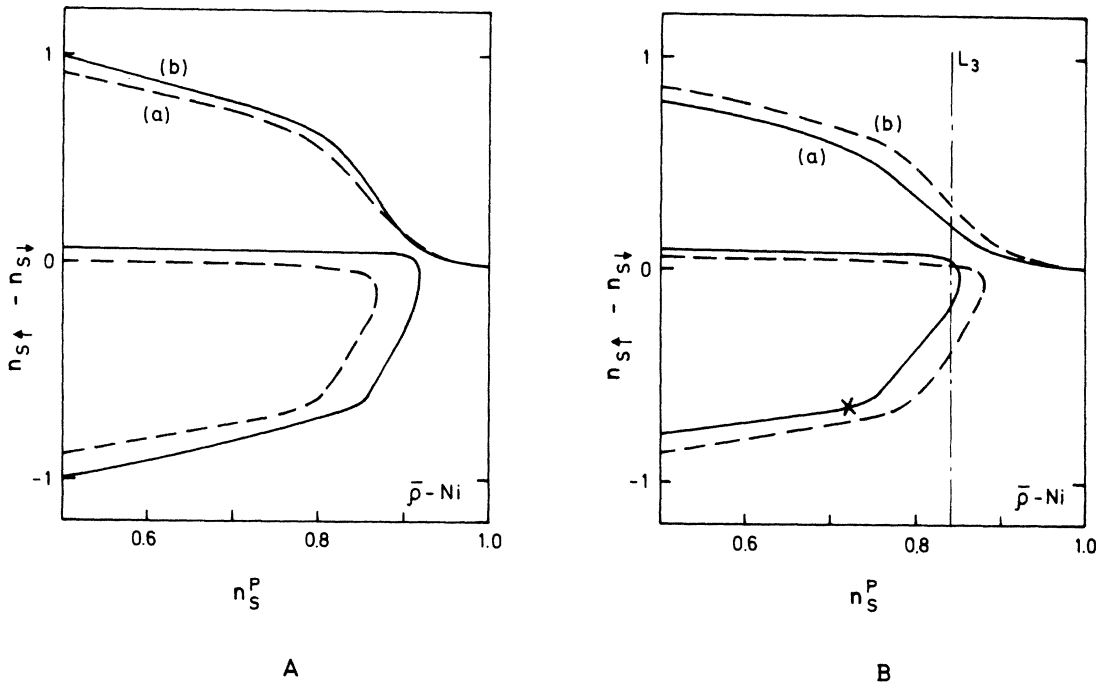

FIG. 7. Surface magnetization $n_{S\uparrow}-n_{S\downarrow}$ vs n_S^P calculated from $\bar{\rho}_{\alpha\sigma}$. Figure 7(A) gives (a) $U=U_S=U_0$, (b) $U=U_S=1.33U_0$ while Fig. 7(B) gives (a) $U=1.06U_0$, $U_S=0.63\,U$, (b) $U=1.06U_0$, $U_S=0.81\,U$. The surface density of states $\bar{\rho}_{\alpha\sigma}(x)$ for the antiferromagnetic solution indicated by a cross is shown in Fig. 5(B). For case (a) of (B), L_3 indicates at which value of n_S^P we draw the energy versus magnetization curve in Fig. 9.

I and II, that is, the point at which the conditions $\partial\Delta E/\partial n_{S\uparrow}=0$ and $\partial\Delta E/\partial n_{S\downarrow}=0$ are both satisfied.

V. DISCUSSION

In the previous sections, we have investigated the problem of surface magnetism in transition metals, mainly with Ni in mind, within the assumptions pointed out in Sec. II. The present model has some similarity to the one of a magnetic impurity embedded in a magnetic matrix which has been extensively studied.[10] The characteristic features of the surface problem are dominated by the fact that the "impurity atoms" [atoms on the surface are impurities in the sense that U_S differs from U and that E_S in Eq. (6a) is nonzero] form a two-dimensional layer. This implies a weaker condition for the occurrence of resonance states and the broadening of these resonance levels. For the one-impurity problem, the energy comparison between the multiple Hartree-Fock solutions has been recently reported by Kanamori.[11] Except for the difference in the dimensionality of the impurities and for the greater sophistication of his treatment, the energy expressions of the two—that is,

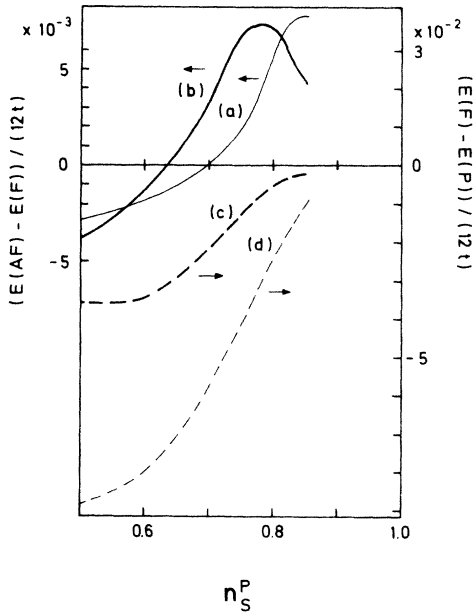

FIG. 8. Energy differences $E(\mathrm{F})-E(\mathrm{P})$ and $E(\mathrm{AF})-E(\mathrm{F})$ evaluated by using $\bar{\rho}_B$ and $\bar{\rho}_{\alpha\sigma}$. Explanation of the various curves is the same as that in Fig. 4.

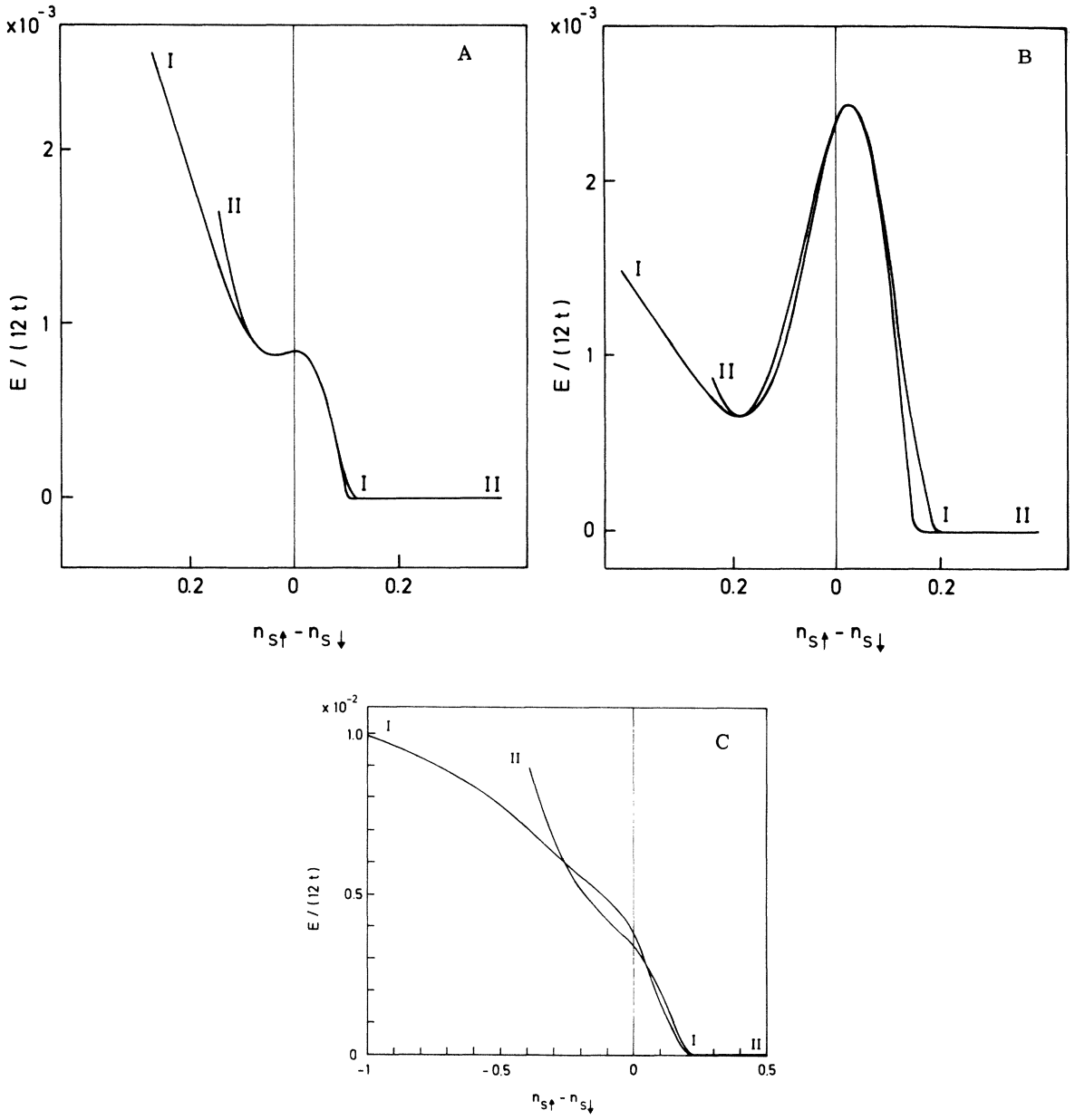

FIG. 9. Energy versus magnetization curves. Curves I are obtained by arbitrarily taking $n_{S\uparrow}$ but calculating $n_{S\downarrow}$ with the condition $\partial\Delta E/\partial n_{S\uparrow} = 0$, while the curves II are obtained by the inverse process (see Appendix B). Parameters U, U_S, and n_S^P are defined by L_1 and L_2 of case (b) of Fig. 3(B) for Figs. 9(A) and 9(B), respectively, and L_3 in case (a) of Fig. 7(B) for Fig. 9(C). Note the energy scale for each figure given in units of the total bandwidth.

Eq. (11) in Ref. 11 and Eq. (21) of the present paper— are quite similar.

We have demonstrated the various possibilities for the surface magnetism depending on the surface parameters U_S and n_S^P, as well as the shape of the bulk density of states. There is one other bulk quantity whose variation is of interest and this is the Fermi energy $\epsilon_{F\sigma}$. Until now we have chosen it such that the number of d holes describes the case of Ni. In order to demonstrate how changes in $\epsilon_{F\sigma}$ influence our previous findings, let us consider fcc Co for which the holes are similarly distributed as for fcc Ni.[12] Assuming the refined density of states $\bar{\rho}_B(x)$ and the strong ferromagnetic limit (that is, one spin band completely filled), we obtain for the magnetization as a function of

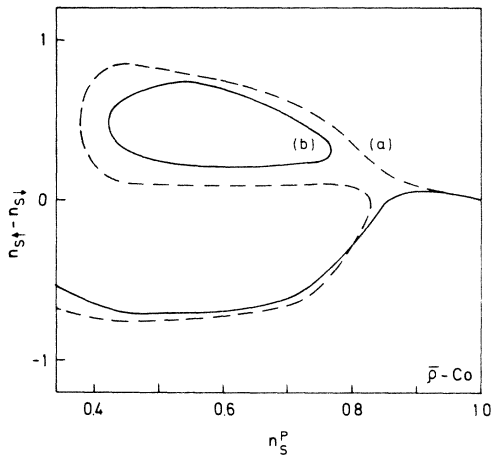

FIG. 10. Surface magnetization $n_{S\uparrow} - n_{S\downarrow}$ vs n_S^P for Co. Shown are (a) $U = U_S = U_0$ and (b) $U = 1.06U_0$, $U_S = 0.81U$. It is emphasized here that in the case (a) $U = U_S = U_0$ the antiferromagnetic solution is lowest in energy in the range $n_S^P \leq 0.71$ (note that three solutions exist in the range $n_S^P \leq n_S^{cr} = 0.76$), while in the case (b) $U = 1.06U_0$ and $U_S = 0.81U$ the antiferromagnetic solution is always lowest in energy.

n_S^P the results shown in Fig. 10. The following parameters were used there: $n_B^P = 0.74$ and $\epsilon_F^P = 1.72$, and, furthermore, $n_{B\uparrow} = 1.0$ and $n_{B\downarrow} = 0.48$ (corresponding to a bulk magnetization of 1.56 μ_B per atom) from which $\epsilon_{F\uparrow} = 3.0 + 3.12(U - U_0)$ and $\epsilon_{F\downarrow} = 1.0$ result. Here $U_0 = 0.61$. Comparing the Co results with those for Ni, one notices that the smaller the values for ϵ_F^P and $\epsilon_{F\downarrow}$, the more the antiferromagnetic solution is preferred. It is worth pointing out, also, that in the Co case the energy difference between the ferromagnetic and the antiferromagnetic solutions is as small as it was calculated for Ni.

Now, we want to make a comment on the low-lying magnetic surface excitation which we found. These correspond to a flip of the surface magnetization from ferromagnetic to antiferromagnetic coupling to the bulk or vice versa. If a material has suitable values for U, U_S, and n_S^P, the excitation energy may be lower than the Curie temperature, as was emphasized in Secs. III and IV. Then the question arises of whether the paramagnetic state, which is highest in energy (see Fig. 9), should be interpreted as a potential barrier between the two minima. If this is the case, then a flip of the surface magnetization is observed as a thermal activation process. If it is not the case (or if the barrier energy is sufficiently small as in the range $n_S^P \simeq n_S^{cr}$), we expect that the magnetization of the surface disappears at much lower temperatures than the bulk Curie temperature.

In order to understand the behavior of surfaces of realistic crystals, it is necessary but not sufficient to know U_S and n_S^P accurately since there are several features not included in our model which should be taken into account. The occupational number n_S^P has been estimated in paper I for Ni by using the renormalized atom approach.[2] For a more accurate determination of n_S^P, several refinements should be considered. Among them is a better estimation of the distortion of the d-electron wave functions near the surface. This is also important for a determination of the intra-atomic Coulomb integral at the surface, i.e., the parameter U_S. However, these problems are beyond the scope of this article, and U_S and n_S^P are therefore left as free parameters.

Not included in our model are realistic lattice structures applicable to Ni or Co (fcc, hcp), interactions extending beyond nearest neighbors, and a possible lattice distortion close to the surface. Furthermore, there is the problem of the extension of surface effects into the bulk.

Several authors, such as Kalkstein and Soven[4] and Haydock and Kelly,[13] have investigated the spatial variation of the electron density of states due to the surface in terms of the tight-binding approximation. According to them, surface effects are insignificant if one penetrates more than two layers into the bulk. It is of interest to compare their results for the surface density of states with the present ones, i.e., $\rho_{\alpha=0}$ in Fig. 1 and $\bar{\rho}_{\alpha=0}$ in Fig. 5(A). One can see that the present results show the qualitative nature of the surface density of states pointed out in Ref. 4, that is, a drastic modification of the Van Hove singularities characteristic of bulk crystalline ρ_B and a decrease of the rms bandwidth.[14] We expect, therefore, that our assumption (iv) of Sec. II A, which neglects any spatial variation of physical quantities except for the surface layer, may be reasonable as far as the surface density of states and the qualitative behavior of $n_{S\sigma}$ are concerned.

However, the spatial variation of physical quantities near the surface may be of importance in a different context. The Hartree-Fock solutions which we obtained are associated with charge accumulation at the surface. This additional charge will be screened out within a few layers from the surface. Also, the deviation of the spin polarization from the bulk value will be appreciable on layers near the surface. This may lead to quantitative changes in the energies of the different surface solutions. At present we find it very hard to investigate these changes rigorously.

Magnetic surface states may have some relevance in interpreting recent photoemission[15] and tunneling[16] experiments on ferromagnetic Ni, Co, and Fe. For example, if the escape depth of photo-

electrons is less than 20 Å, as it was noted in Ref. 15, then surface effects should play an important role. Our findings show it to be quite likely that in this case the measured quantities can appreciably deviate from those of the bulk.

VI. SUMMARY AND CONCLUSIONS

We have made an energy comparison between the different Hartree-Fock solutions which occur in the magnetic surface problem of transition metals. The parameters were chosen to describe as well as possible the case of Ni. The conditions were worked out under which an antiferromagnetic surface solution has the lowest energy. We have also studied how sensitive our results are to the chosen form of the bulk density of states. Attention was drawn to low-lying magnetic surface excitations which correspond to a flip of the surface layer from ferromagnetic to antiferromagnetic coupling to the bulk or vice versa.

APPENDIX A: SURFACE DENSITY OF STATES

The calculation of Eq. (25) is straightforward and $\rho_\alpha^{\mathrm{NR}}(x)$ is given by

$$2t\rho_\alpha^{\mathrm{NR}}(x)=\begin{cases}\gamma_\alpha - f_\alpha(\arccos(x+2)), & -3<x\le -1\\ \gamma_\alpha, & -1<x\le 1\\ f_\alpha(\arccos(x-2)), & 1<x<3,\end{cases} \tag{A1}$$

where

$$\gamma_\alpha=\begin{cases}\frac{1}{4}, & |\alpha|<1\\ \frac{1}{4}\alpha^{-2}, & |\alpha|>1,\end{cases}$$

and

$$f_\alpha(\theta)=\frac{1}{4\pi\alpha}\left[\frac{1+\alpha^2}{2\alpha}\theta+\sin\theta - \frac{1-\alpha^2}{\alpha}\arctan\left(\frac{1+\alpha}{1-\alpha}\tan\frac{\theta}{2}\right)\right].$$

For the case $|\alpha|>1$, the spectral weight is divided as

$$2t\int_{-\infty}^{\infty}dx\,\rho_\alpha^{\mathrm{NR}}(x)=\alpha^{-2}$$

and

$$2t\int_{-\infty}^{\infty}dx\,\rho_\alpha^{\mathrm{R}}(x)=1-\alpha^{-2}.$$

If physical quantities are calculated by using the density of states $\bar\rho_{\|}$, it is only necessary to rewrite the y integration, such as the one in Eq. (25), as

$$\tfrac{1}{8}\int_{-2}^{2}dy \to b\int_{-2}^{\beta}dy + a\int_{\beta}^{2}dy,$$

where a and b are defined in Eq. (27). This change does not introduce any difficulty in the explicit calculations, although it makes the final results look more complicated.

APPENDIX B: ENERGY CALCULATION

Using the various energy units introduced in the text, Eq. (21) reduces to

$$\frac{\Delta E}{tN_{\|}}=-\frac{4t}{\pi}\sum_\sigma \mathrm{Im}\int_{-\infty}^{\epsilon_{F\sigma}}dx(x-\epsilon_{F\sigma})\int_{-2}^{+2}dy\,\rho_{\|}(y) \times\frac{\partial}{\partial x}\ln[G_\sigma(x,y;0,0)^{-1}]-12U_S n_{S\uparrow}n_{S\downarrow}. \tag{B1}$$

From Eqs. (11)–(13), the relation

$$\frac{\partial}{\partial x}G_\sigma(x,y;0,0)=-\frac{\partial}{\partial y}G_\sigma(x,y;0,0)$$

is derived. Then, substituting the density of states of Eq. (23) into $\rho_{\|}(y)$, we can at once carry out the y integration. We obtain

$$\begin{aligned}\frac{\Delta E}{tN_{\|}}&=\frac{1}{2\pi}\sum_\sigma \mathrm{Im}\int_{-\infty}^{\epsilon_{F\sigma}}dx(x-\epsilon_{F\sigma})\ln\left(\frac{G_\sigma(x,2;0,0)^{-1}}{G_\sigma(x,-2;0,0)^{-1}}\right)\\ &\quad -12U_S n_{S\uparrow}n_{S\downarrow}\\ &\equiv\sum_\sigma[\delta E(\epsilon_{F\sigma}-2,\alpha_\sigma)-\delta E(\epsilon_{F\sigma}+2,\alpha_\sigma)]\\ &\quad -12U_S n_{S\uparrow}n_{S\downarrow},\end{aligned} \tag{B2}$$

where $\alpha_\sigma=E_{S\sigma}/t$ and

$$\delta E(\gamma,\alpha)=\frac{1}{2\pi}\int_{-\infty}^{\gamma}d\xi(\xi-\gamma)\,\mathrm{Im}\{\ln[(\xi^2-1)^{1/2}+\xi-\alpha]\}. \tag{B3}$$

Here we have used the following explicit form for $G_\sigma(x,y;0,0)$:

$$G_\sigma(x,y;0,0)=t/[(\xi^2-1)^{1/2}+\xi-\alpha_\sigma], \tag{B4}$$

where $\xi=(x-y)$. The correct branch of the logarithms in Eq. (B3) is determined by the fact that the (retarded) Green's function (B4) always has a negative imaginary part. Then in the case $\alpha>1$, for example, the function $\mathrm{Im}\{\ln[(\xi^2-1)^{1/2}+\xi-\alpha]\}$ is equal to π for $\xi\le -1$ and $1\le\xi<x_c$, and equal to 0 for $\xi>x_c$, where $x_c=(\alpha^2+1)/(2\alpha)$. When $-1<\xi<1$, the function varies between π and $\pi/2$. This discontinuity at $\xi=x_c$ corresponds to a surface resonance level. In the case $\alpha<-1$, the discontinuity occurs at $\xi=x_c<-1$, while in the case of $-1<\alpha<1$ there is no discontinuity. Explicit calculation of Eq. (B3) is then straightforward. Here we only write the final result for the range $\alpha\le 1$ and $\gamma>1$, and $\alpha>1$ and $\gamma>x_c$:

$$\delta E(\gamma,\alpha)=\tfrac{1}{8}-\tfrac{1}{4}\alpha\gamma+\tfrac{1}{16}\alpha^2. \tag{B5}$$

Within our model, the contribution to ΔE from electrons in the surface doublet substates is evaluated in a similar manner. We only have to reinterpret α_σ and $\epsilon_{F\sigma}$ properly. The assumption (iii) of Sec. II A that the doublet states are completely filled requires a small α_σ and $\epsilon_{F\sigma} > 3$ for these states. Therefore, we can use Eq. (B5) for both $\gamma = \epsilon_{F\sigma} - 2$ and $\epsilon_{F\sigma} + 2$. We can see at once that the first term in Eq. (B2) exactly cancels the second term when we only consider the contributions coming from these substates. [Note that in this case the second term is given by

$$-24U_S \sum_\sigma n_{D\sigma} n_S = -48U_S n_S,$$

where $n_{D\sigma}(=1)$ is the occupation number of one of the doublet states. The surface potential α is given by

$$\alpha = E_D + 12U_S n_S,$$

where $E_D = \tilde{E}_D/t$.] Thus, we can justify the assumption made in Sec. II.

It is interesting to look at the energy of different states which are not Hartree-Fock states, that is, states for which the HF conditions $2\Delta E/\partial n_{S\uparrow} = 0$ and $\partial \Delta E/\partial n_{S\downarrow} = 0$ are both satisfied. Such a calculation is possible if we use Eq. (B2), which contains only $n_{S\sigma}$ and $\epsilon_{F\sigma}$ as parameters. [Here we implicitly assume that the effective potentials are given by Eq. (6a) even when $n_{S\sigma}$ is arbitrary.] In fact, we calculate the energy versus magnetization curves shown in Fig. 9 as follows: First we take an arbitrary value for $n_{S\uparrow}$, determine $n_{S\downarrow}$ by one of the two HF conditions $\partial \Delta E/\partial n_{S\uparrow} = 0$, and evaluate ΔE using Eq. (B2). This way we obtain curve I. For curve II, $n_{S\downarrow}$ is chosen arbitrarily. It is worth noting here the flatness at one end of curve II. In this range, the condition $\partial \Delta E/\partial n_{S\downarrow} = 0$ gives rise to $n_{S\uparrow} = 1$ for different values of $n_{S\downarrow}$. This indicates the fact that if the up-spin band is always filled, ΔE is independent of the down-spin occupation number $n_{S\downarrow}$ when we remove the condition $\partial \Delta E/\partial n_{S\uparrow} = 0$. This situation is the same as the independence of energy from the filled doublet states discussed just before.

---

*Supported in part by Deutsche Forschungsgemeinschaft.

†Present address of the authors: Max-Planck-Institut für Festköperforschung, (7) Stuttgart, Germany.

[1]P. Fulde, A. Luther, and R. E. Watson, Phys. Rev. B 8, 440 (1973).

[2]L. Hodges, R. E. Watson, and H. Ehrenreich, Phys. Rev. B 5, 3953 (1972).

[3]T. Moriya, in *Proceedings of the International School of Physics "Enrico Fermi," Course 37*, edited by W. Marshall (Academic, New York, 1967).

[4]D. Kalkstein and P. Soven, Surf. Sci. 26, 85 (1971).

[5]D. Mills, M. T. Beal-Monod, and R. A. Weiner, Phys. Rev. B 5, 4637 (1972).

[6]By "feedback effects" we mean here the modification of bulk properties due to the perturbation on the surface H^S. For example, H^S changes the bulk density of states, so that the energy of the electrons inside the bulk varies when $n_{S\sigma}$ changes. Such an effect is taken into account in Eq. (21).

[7]A. A. Abrikosov, L. P. Gor'kov, and I. E. Dzyaloshinski, *Method of Quantum Field Theory in Statistical Physics*, (Pergamon, New York, 1965), Sec. 15.

[8]Note that we measure the electron energy from the center of the bulk band for each spin direction.

[9]See, for example, L. Hodges, H. Ehrenreich, and N. D. Lang, Phys. Rev. 152, 505 (1966).

[10]See, for example, Ref. 3 and references therein; also see I. A. Campbell and A. A. Gomès, Proc. Phys. Soc. Lond. 91, 319 (1967).

[11]J. Kanamori, lecture presented in the Conference on the Disordered Metals, Strasbourg, 1973, J. Phys. (to be published).

[12]L. Hodges and H. Ehrenreich, J. Appl. Phys. 39, 1280 (1968).

[13]R. Haydock and M. J. Kelly, Surf. Sci. 38, 139 (1973).

[14]F. Cyrot-Lackmann, J. Phys. Chem. Solids 29, 1235 (1968).

[15]G. Busch, M. Campagna, and H. C. Siegmann, Phys. Rev. B 4, 746 (1971); G. Busch, M. Campagna, D. T. Pierce, and H. C. Siegmann, Phys. Rev. Lett. 28, 611 (1972).

[16]P. M. Tedrow and R. Merservey, Phys. Rev. B 7, 318 (1973).